Adaptation rate in joint dynamics depends on the time-varying properties of the environment

Van De Ruit, Mark; Lataire, John; Van Der Helm, Frans C.T.; Mugge, Winfred; Schouten, Alfred C.

DOI
10.1109/BIOROB.2018.8487793

Publication date
2018

Document Version
Final published version

Published in
BIOROB 2018 - 7th IEEE International Conference on Biomedical Robotics and Biomechatronics

2018 7th IEEE International Conference on Biomedical
Robotics and Biomechatronics (Biorob)
Enschede, The Netherlands, August 26-29, 2018

Adaptation rate in joint dynamics depends on the time-varying properties of the environment*

Mark van de Ruit, John Lataire, *Member, IEEE*, Frans C. T. van der Helm, Winfred Mugge and Alfred C. Schouten

***Abstract*— During movement, our central nervous system (CNS) takes into account the dynamics of our environment to optimally adapt our joint dynamics. In this study we explored the adaptation of shoulder joint dynamics when a participant interacted with a time-varying virtual environment created by a haptic manipulator. Participants performed a position task, i.e., minimizing position deviations, in face of continuous mechanical force perturbations. During a trial the environmental damping, mimicked by the manipulator, was either increased (0 to 200 Ns/m) or decreased (200 to 0 Ns/m) in 1 s or 8 s. A system identification technique, kernel-based regression, was used to reveal time-varying shoulder joint dynamics using the frequency response function (FRF). The FRFs revealed that the rate at which shoulder joint dynamics is adapted depends on the rate and direction of change in environmental damping. Adaptation is slow, but starts immediately, after the environmental damping increases, whereas adaptation is fast but delayed when environmental damping decreases. The results obtained in our participants comply with the framework of optimal feedback control, i.e., adaptation of joint dynamics only takes place when motor performance is at risk or when this is energetically advantageous.**

I. Introduction

Successful performance of skilled movement relies on the ability of the human central nervous system (CNS) to adequately predict joint dynamics that is required to successfully interact with the environment. Moreover, it is important joint dynamics can be rapidly adapted when unexpected changes in environmental dynamics occur. An important way by which the CNS facilitates rapid adaptations in joint dynamics is by making use of reflexes. Reflexes are not just simple input-output responses of the CNS, but are intricate responses which share many sophisticated properties with voluntary human motor control [1]. Hence, the strength of the human reflex feedback pathways is context dependent and tuned such that movement goals can be achieved effortlessly and external disturbances can be easily counteracted [2].

Reflexes are rapid involuntary muscle responses which together with the muscle's intrinsic properties determine the dynamics of a joint [3]. Reflexes are often studied by applying brief rapid stretches to a muscle, resulting in a characteristic response in muscle activity. In the upper extremities this response is composed of a short and long latency peak. The short latency response (SLR) is considered to be spinal of origin, whereas for the long latency response (LLR) may also involve cortical processes [4]. The latter has been concluded based on observations that the LLR, but not the SLR, changes with behavioural context, e.g., participant intent [5], dynamics of the environment [6], and task goals [7]. For example, participants tend to reduce reflex strength when interacting with a stiff compared to a compliant virtual environment [8].

System identification (SI) can be used to quantify and separate intrinsic and reflexive contributions to joint dynamics during posture and movement [9, 10]. SI is often employed under the assumption that joint displacements are small and acting around a single working point, allowing the application of linear time-invariant (LTI) techniques either in time- or frequency domain. However, when interested in studying joint dynamics during movement, linear time-varying (LTV) or linear parameter varying (LPV) techniques are required, as joint dynamics changes with e.g. joint position and torque [11-13]. Whereas both LPV and LTV techniques have been successfully employed to quantify joint dynamics during movement [14-16], up until now this has only been done when participants adapted joint torque or position using a predefined pattern. It is still to be elucidated how joint dynamics is adapted when unexpected changes, e.g., in the environment, put motor performance at risk.

In this pilot study we demonstrate how a novel LTV SI method, kernel-based regression (KBR) [17], is used to study the rate of adaptation in shoulder joint dynamics. Participants interact with a time-varying virtual environment while performing a position task [18]. Adaptation in joint dynamics is required when an unexpected change in environmental damping is presented, such that the participant experiences either a transition from an environment with low (0 Ns/m) to high damping (200 Ns/m) or from high (200 Ns/m) to low damping (0 Ns/m). It is hypothesized that joint dynamics is most rapidly adapted when moving from a high to low damping environment as an immediate risk to motor performance occurs.

* This research was funded by the European Research Council under the European Union's Seventh Framework Programme (FP/2007-2013) ERC Grant Agreement n. 291339, project 4DEEG: A new tool to investigate the spatial and temporal activity patterns in the brain. John Lataire is supported in part by the Flemish Government (Methusalem) and the Belgian Government through the Inter university Poles of Attraction (DYSCO) Program.

Mark van de Ruit, Frans C. T. Van der Helm, Winfred Mugge and Alfred C. Schouten are with the Laboratory for Neuromuscular control, Department of Biomechanical Engineering, Delft University of Technology, Mekelweg 2, 2628CD, Delft, The Netherlands (e-mail: m.l.vanderuit-1@tudelft.nl; f.c.t.vanderhelm@tudelft.nl; w.mugge@tudelft.nl; a.c.schouten@tudelft.nl)

John Lataire is with the Department of Electrical Engineering, Vrije Universiteit Brussel, 1050 Brussels, Belgium (e-mail: John.Lataire@vub.be)

978-1-5386-8183-1/18/$31.00 ©2018 IEEE

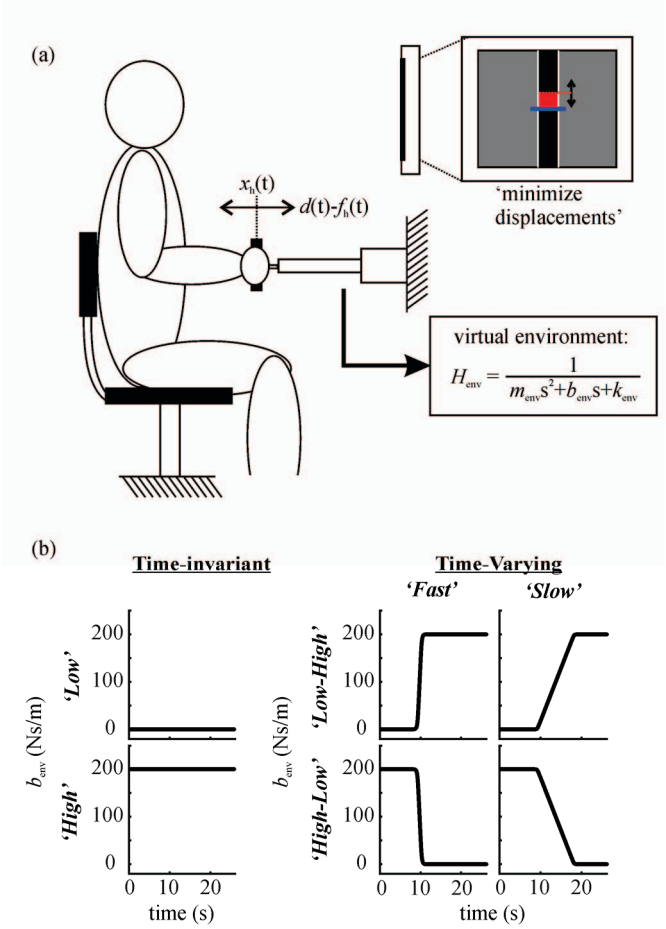

Fig 1. Overview of the experimental setup and experimental conditions. (a) A hydraulic manipulator was used to apply force perturbations to the hand of the participant along the sagittal plane in posterior-anterior direction, effectively rotating the shoulder, that was interacting with a virtual environment behaving as a mass-spring-damper system. The arm was aligned with the piston of the manipulator such that the elbow was at a 90 deg angle making any rotation of the elbow ineffective in counteracting the perturbation. A force perturbation d(t) was applied to the handle of the manipulator while recording the handle position x_h(t) and force applied to the handle f_h(t) (b) Environmental damping (b_{env}) was varied across six conditions. Two time-invariant conditions (left), with either a low (0 Ns/m) or high damping (200 Ns/m), and four time-varying conditions (right) where damping changes during the trial from either low to high, or high to low, damping in1 s ('fast') or 8 s ('slow').

II. Experimental Methods

A. Participant

Five healthy participants (4 men; 29±5 years, 1 woman; 24 years), with no self-reported history of neurological or orthopedic arm problems, participated in the experiment. All participants were right handed. The study protocol was approved by the human research ethics committee (HREC) of Delft University of Technology, and all participants provided written informed consent before participating.

B. Experimental Setup

A force-controlled hydraulic linear manipulator applied force perturbations to the hand of the participant [19]. The piston only allows displacements of the handle along the sagittal plane in posterior and anterior direction. The forearm

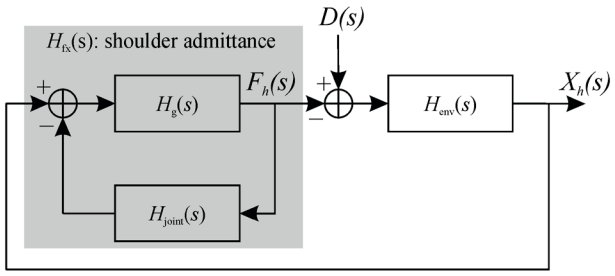

Fig 2. Representation of the shoulder joint dynamics H_{fx}(s) in conjunction with the virtual environment of the manipulator H_{env}(s). The shoulder dynamics is modelled by the grip dynamics H_g(s) and joint intrinsic properties H_{joint}(s). Force F_h(s), position X_h(s) and the applied perturbation D(s) are measured.

of the participants was aligned with the piston of the manipulator (90 deg elbow angle) and participants were instructed to maintain a firm grip during all trials. A force transducer (SENSOTEC – Model 31E – 100N0 – 1DOF) measured the interaction force between the hand of the participant and the manipulator in line with the direction of displacement of the handle (anterior-posterior direction). Because the hand was moved only in the anterior-posterior direction, rotations of the shoulder and elbow were interdependent and displacements of the hand can be related to rotations of the shoulder joint (Fig. 1a). Hence, rotations of the elbow are ineffective in counteracting any perturbations but are not explicitly restricted by the experimental setup.

Throughout the experiment, participants minimized the displacements of the manipulator's handle while continuous force perturbations were applied. A monitor was used to provide feedback on the position of the handle of the manipulator with respect to the target (reference) position.

A block scheme representing the interaction between joint and environmental dynamics is given in Fig. 2. The participants perceived the manipulator as an interaction with a mass-spring-damper system (H_{env}) of which the parameters are adjustable. In this study, the mass (m_{env}) was kept constant at a value of m_{env} = 1 kg, and no virtual spring was used (k_{env} = 0 N/m). The virtual damping (b_{env}) was varied during and between trials to provoke time-varying changes in shoulder joint admittance.

C. Measurement Protocol

Each participant completed 36 trials, divided over six conditions and each trial lasted 35 s. In two conditions the virtual damping of the manipulator was time-invariant, while in the remaining four conditions the damping varied during the trial. For the time-invariant conditions, damping (b_{env}) was set to either 0 Ns/m or 200 Ns/m. Damping was changed from 0 to 200 Ns/m or 200 to 0 Ns/m during the time-varying conditions. The transition was made in either 1 s or 8 s. The conditions are summarized in Fig. 1b. Presentation of conditions was pseudo-random and participants were not informed about which condition was presented. All data was acquired with a sample frequency of 2500 Hz.

D. Perturbation signal design

To improve the signal-to-noise ratio and to allow the detection of relevant joint dynamics – random phase multisine force perturbations were applied to the hand. The multisine perturbation is defined as:

$$u(t) = \sum_{k_e \in \mathbb{K}_{exc}} A_{k_e} \cos(\omega_{k_e} t + \phi_{k_e}) \quad (1)$$

Thus, the multisine signal is a sum of cosines, with

- angular frequencies $\omega_{k_e} = 2\pi k_e / T$, where T is the period length (in s) of the multisine signal,
- $\mathbb{K}_{exc} \subset \mathbb{N}$ a sparse set of excited frequency bins, chosen sufficiently separated to ensure the identifiability of the model (as elaborated in [20]).
- amplitudes A_{k_e}, which, in concordance with $\mathbb{K}_{exc}$, determine the spectral content of the perturbation.
- phases ϕ_{k_e}, which are chosen randomly, uniformly distributed from $[0, 2\pi[$.

In this experiment the multisine perturbation had a period of $T = 2^{15}$ samples (~13 s). As a result, each trial consisted of two full periods of the multisine and part of the multisine to fill the 35 s for each trial. The perturbation signal was designed to justify the use of linear model approximations by keeping the position deviations small around the working-point of the shoulder. Therefore, at the start of each experiment the force perturbation was scaled such that the displacement of the handle had a root mean square (RMS) value of ~3 mm for both time-invariant damping conditions (0 and 200 Ns/m) for every participant. This means that during the time-varying conditions, the perturbation signal was scaled online along with the time-varying environmental damping. The perturbation signal had a bandwidth of 0.5-20 Hz, with equal power across all excited frequencies (Fig. 3a). These characteristics of the multisine perturbation signal (1) have been chosen based on previous research to allow characterizing all relevant shoulder dynamics and ensure the total system can be assumed to behave linearly [19].

E. Data processing and analysis

Data of all trials and participants was processed individually. As a result data presented is always single trial data from a single participant.

Pre-Processing: Before further processing the first ~ 9 s of the each trial in each participants was removed to ensure that any initial transient effects would not affect the results. The remaining 2^{16} samples (~ 26 s) of data, comprising two periods of the multisine was used for further analysis.

Time-invariant system identification: Conventional linear time-invariant (LTI) system identification was performed on the data recorded during the time-invariant conditions [9, 19]. Recorded signals were averaged in time domain across trials to minimize the variance due to noise in the signals. Subsequently, the fast Fourier transform (FFT) was used to transform the averaged signals to the frequency domain.

A spectral estimator for closed loop systems was employed to account for the interacting dynamics of the joint and the virtual environment (Fig. 2). Mechanical joint admittance $\hat{H}_{fx}(f)$ was determined by estimating the frequency response function (FRF) using:

$$\hat{H}_{fx}(f) = \frac{\hat{S}_{dx}(f)}{\hat{S}_{df}(f)} \quad (2)$$

where $\hat{S}_{dx}(f)$. is the estimated cross spectral density between $d(t)$ and $x_h(t)$ and $\hat{S}_{df}(f)$. is the estimated cross spectral density between $d(t)$ and $f_h(t)$.

Time-variant system identification: The parametric identification technique proposed in [17] for linear time-variant systems was used to quantify joint dynamics during the time-varying conditions. This method assumes that the system's input and output signals, in this case $f_h(t)$ and $x_h(t)$, satisfy the following linear differential equation:

$$x_h(t) = -\sum_{n=1}^{N_a} a_n(t) \frac{d^n x_h(t)}{dt^n} + \sum_{n=0}^{N_b} b_n(t) \frac{d^n f_h(t)}{dt^n} \quad (3)$$

The coefficients to be estimated, $a_n(t)$ and $b_n(t)$, are functions of time and, thus, allow for time-varying properties of the estimated dynamics. They are estimated via kernel-based regression. This implies that the cost function to be minimized includes a regularization term which imposes a structure on the estimated coefficients. This regularization term is the squared norm of these coefficients in the reproducing Kernel Hilbert space, induced by a chosen kernel. For this work, the squared exponential radial basis function (RBF) kernel is used, given by:

$$K(t, t') = \gamma e^{\frac{-(t-t')^2}{\sigma^2}}, \quad t, t' = 0, T_s, \dots, (N-1)T_s \quad (4)$$

with hyperparameters σ and γ determing the properties of the kernel. The RBF kernel is known to impose smoothness on the estimated coefficients which is determined by σ (higher σ results in a higher smoothness), while γ is a regularization parameter which allows to tune the trade-off between the bias and the variance on the estimated parameters.

The estimator is formulated in the frequency domain: the estimate minimizes the sum of i) the squared norm of the *spectral* difference between the left and right hand side of (3) in the frequency band of interested, and ii) the regularization term to impose the structure on the estimated coefficients. For the purpose of this study, we assumed $\sigma = \sim 5$ s and $\gamma = 6 \cdot 10^{-4}$.

Fig. 2 shows that the total shoulder admittance $\hat{H}_{fx}(s)$ is composed of the dynamics of the shoulder joint $H_{joint}(s)$ and the grip dynamics $H_g(s)$, representing the interaction between hand and manipulator. The joint and grip dynamics are assumed to be represented by the following systems [18]:

$$H_{joint}(s) = \frac{1}{Is^2 + bs + k} \quad (5)$$

$$H_g(s) = b_c s + k_c \quad (6)$$

in which s is the Laplace variable and equals $j2\pi f$ (f represents the frequency) when evaluated on the imaginary axis. $H_{joint}(s)$ represents the intrinsic and reflexive joint dynamics where I is the limb inertia, b the joint viscosity and

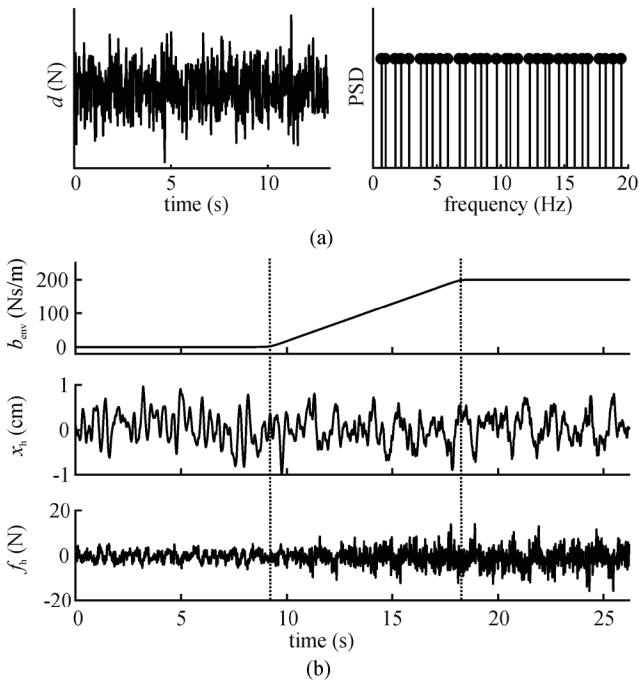

Fig 3. Raw data records. (a) The multisine force perturbation signal in time (left) and frequency domain. Frequencies between 0.5 – 20 Hz were excited. (b) (top) The time-varying damping across the trial during which the environmental damping changed from low-high in 8 s. Raw position (middle) and force data (bottom) for a representative trial.

k the joint stiffness. $H_g(s)$ represents the grip dynamics, a simple spring-damper system where b_c is the contact viscosity and k_c the contact stiffness.

The overall system representing the mechanical joint admittance from joint torque ($F_h(s)$ – and taken equivalent to the position of the handle of the manipulator) to joint position $X_h(s)$ is then:

$$H_{fx}(s) = \frac{1 + H_{joint}(s)H_g(s)}{H_g(s)} \tag{7}$$

$$= \frac{Is^2 + (b + b_c)s + (k + k_c)}{Is^3 + (b_c b + k_c I)s^2 + (b_c k + k_c b)s + kk_c}$$

Therefore, to comply with the model structure in Eq. (7) the order of N_a and N_b in Eq. (3) was chosen as 3 and 2 respectively.

Low-frequency admittance: A single joint property was extracted from the time-varying FRF and defined as the low-frequency admittance, representative for the inverse of the joint stiffness. The low-frequency admittance was determined as the average joint admittance across the frequency range of 0.5-2 Hz. This measure is used to reveal adaptations in joint admittance over time when faced with changing environmental conditions.

III. Results

Data from a single representative participant is presented. Hence, data from all other participants demonstrated similar trends and main effects. Fig. 3b shows raw hand position and force data for a single trial during which the damping was changed from 0 to 200 Ns/m.

LTI system identification was used to study the two time-invariant conditions (Fig. 4). For this participant, the primary differences are a higher resonance peak, and lower admittance at low frequencies, when there is a higher environmental damping (200 Ns/m).

An example of a time-varying FRF is provided in Fig. 4 (lower panel). In this trial, damping was changed from 0 to 200 Ns/m in 8 s, starting after ~9s in the trial. Consequently, a slow reduction in admittance at the low frequencies is observed up to a new 'steady state'. For all conditions, and all trials, the mean admittance across the frequency range 0.5-2 Hz ('low-frequency admittance') is visualized in Fig. 5. Adaptation is fast but delayed with respect to the onset of change in damping, when damping is changed from 200-0 Ns/m, whereas slow but immediate adaptation is observed for damping 0-200 Ns/m conditions.

IV. Discussion

This pilot study demonstrates that the tested healthy participants can flexibly tune their joint dynamics under changing environmental properties.

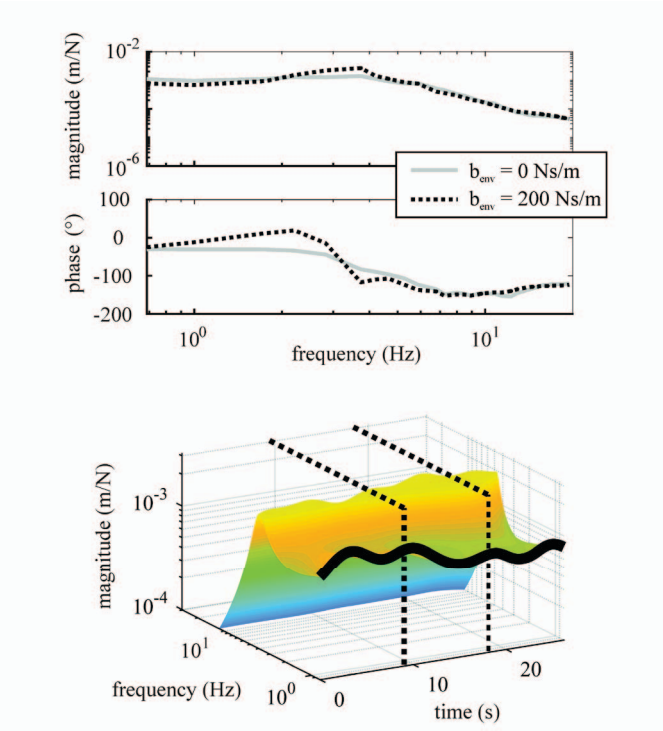

Fig 4. Data of a single trial in a representative participant (top) Frequency response functions (FRFs) - $X_h(s)/F_h(s)$ - magnitude and phase, for the two time-invariant conditions. (bottom) Magnitude of the frozen FRF across the full trial where the damping was changed from low-high (0 to 200 Ns/m) in 8 s (start and end of transition indicated by dashed black lines). The black solid line represents the admittance at the lowest frequency (~0.5 Hz) and demonstrates the time-varying admittance.

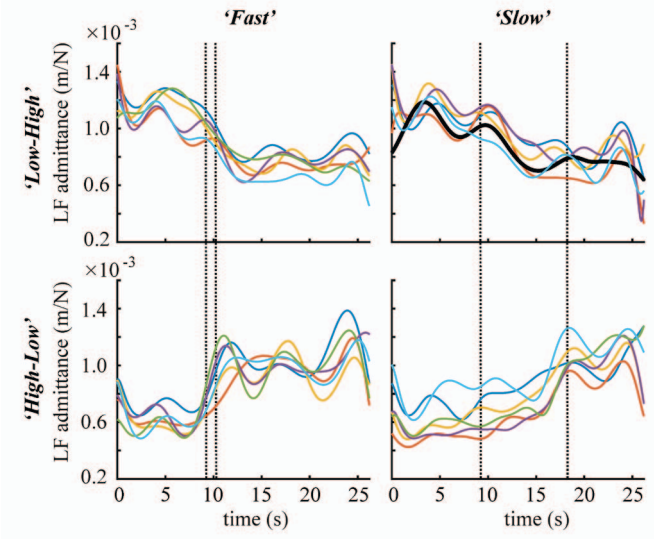

Fig 5. The low-frequency magnitude of the admittance FRF for the 6 trials of each time-varying condition of a single participant. The black line (top right panel) represents the same time-varying trial as in Fig. 4.

The delay and rate of adaptation with which joint dynamics is adapted following a change in environmental damping depends on both the speed and direction of change, i.e. whether the environment provides more or less damping.

In line with our hypothesis, joint dynamics is most rapidly adapted when a change from a high (200 Ns/m) to low damping (0 Ns/m) environment occurred. This contrasts the slower adaptation when moving from a low to a high damping environment. Moreover, the onset of adaptation is later when the environment initially has a high damping compared to when having a low damping.

While results should be interpreted with care, provided the low number of participants, they are supportive to the theory of optimal feedback control (OFC). OFC has been successfully used in voluntary motor control to explain changes in control behaviour by weighing costs (i.e., energy expenditure) and benefits (motor performance) [2, 21, 22]. In a position task it is assumed the CNS controls stability of the total system, the joint together with the environment, and continuously adapts joint dynamics to optimally function in the environment experienced [18]. However, adaptation will only occur when this is energetically advantageous and improves motor performance. Hence, when transitioning from an environment with high to low damping, there is only need to adapt joint dynamics when there is risk of the total system becoming unstable. This occurs much later in the 8 s transition than the 1 s transition. Likewise, when transitioning from an environment with low to high damping, stability of the joint can be reduced without affecting performance but reducing energetic demand. The latter can be achieved by increased use of reflexes rather than co-contraction. Reflexes have an inherent time delay which results in oscillations and a higher resonance peak [18]. This is no risk to motor performance when the environment provides damping of these oscillations. It can be concluded that for the participants in this study, there exists a trade-off between the speed by which joint mechanics is adapted and the risk for the total system to become unstable.

Humans can regulate their joint dynamics by using either co-contraction or reflexes when interacting with time-varying environments [6, 23, 24]. An increased use of reflexes has been used to explain the changes in joint dynamics when performing a position task in an environment with high damping (b_{env} = 200 Ns/m) compared to when performing the same task in an environment with low damping [18]. This has been concluded from the increase in the resonance peak when moving to an environment providing more damping and the reduced admittance (higher stiffness) at low frequencies, reducing the joint's sensitivity to joint perturbations (Fig. 4). Based on these results, it is reasonable to assume that for the participants tested in this pilot study, changes in reflex strength underlie the observed time-varying joint dynamics.

Future work should extend these results to a larger sample size, validate the adopted model orders and hyperparameters and quantify the intrinsic and reflexive contributions to the observed adaptation in joint dynamics. This will open up the way to further explore how the CNS controls our joint dynamics and how CNS damage impairs movement control.

ACKNOWLEDGMENT

The authors like to thank Henri Boessenkool for his help with programming and maintenance of the haptic manipulator.

REFERENCES

[1] S. H. Scott, "The computational and neural basis of voluntary motor control and planning," *Trends Cogn Sci,* vol. 16, pp. 541-9, Nov 2012.

[2] D. Liu and E. Todorov, "Evidence for the flexible sensorimotor strategies predicted by optimal feedback control," *J Neurosci,* vol. 27, pp. 9354-68, Aug 29 2007.

[3] T. Sinkjaer, E. Toft, S. Andreassen, and B. C. Hornemann, "Muscle stiffness in human ankle dorsiflexors: intrinsic and reflex components," *J Neurophysiol,* vol. 60, pp. 1110-21, Sep 1988.

[4] P. B. Matthews, "The human stretch reflex and the motor cortex," *Trends Neurosci,* vol. 14, pp. 87-91, Mar 1991.

[5] J. G. Colebatch, S. C. Gandevia, D. I. McCloskey, and E. K. Potter, "Subject instruction and long latency reflex responses to muscle stretch," *J Physiol,* vol. 292, pp. 527-34, Jul 1979.

[6] E. J. Perreault, K. Chen, R. D. Trumbower, and G. Lewis, "Interactions with compliant loads alter stretch reflex gains but not intermuscular coordination," *J Neurophysiol,* vol. 99, pp. 2101-13, May 2008.

[7] V. Dietz, M. Discher, and M. Trippel, "Task-dependent modulation of short- and long-latency electromyographic responses in upper limb muscles," *Electroencephalogr Clin Neurophysiol,* vol. 93, pp. 49-56, Feb 1994.

[8] J. Shemmell, J. H. An, and E. J. Perreault, "The differential role of motor cortex in stretch reflex modulation induced by changes in environmental mechanics and verbal instruction," *J Neurosci,* vol. 29, pp. 13255-63, Oct 21 2009.

[9] R. E. Kearney and I. W. Hunter, "System identification of human joint dynamics," *Critical reviews in biomedical engineering,* vol. 18, pp. 55-87, 1990.

[10] M. P. Vlaar and A. C. Schouten, "System identification for human motion control," in *2015 IEEE International Instrumentation and Measurement Technology Conference (I2MTC) Proceedings*, 2015, pp. 600-605.

[11] M. M. Mirbagheri, H. Barbeau, and R. E. Kearney, "Intrinsic and reflex contributions to human ankle stiffness: variation with activation level and position," *Exp Brain Res,* vol. 135, pp. 423-36, Dec 2000.

[12] R. E. Kearney and I. W. Hunter, "Dynamics of human ankle stiffness: variation with displacement amplitude," *J Biomech,* vol. 15, pp. 753-6, 1982.

[13] I. W. Hunter and R. E. Kearney, "Dynamics of human ankle stiffness: variation with mean ankle torque," *J Biomech,* vol. 15, pp. 747-52, 1982.

[14] D. Ludvig, M. Plocharski, P. Plocharski, and E. J. Perreault, "Mechanisms contributing to reduced knee stiffness during movement," *Exp Brain Res,* Jul 15 2017.

[15] M. A. Golkar, E. Sobhani Tehrani, and R. E. Kearney, "Linear Parameter Varying Identification of Dynamic Joint Stiffness during Time-Varying Voluntary Contractions," *Front Comput Neurosci,* vol. 11, p. 35, 2017.

[16] J. B. MacNeil, R. E. Kearney, and I. W. Hunter, "Identification of time-varying biological systems from ensemble data," *IEEE Trans Biomed Eng,* vol. 39, pp. 1213-25, Dec 1992.

[17] J. Lataire, R. Pintelon, D. Piga, and R. Toth, "Continuous-time linear time-varying system identification with a frequency-domain kernel-based estimator," *Iet Control Theory and Applications,* vol. 11, pp. 457-465, Feb 2017.

[18] A. C. Schouten, E. de Vlugt, J. J. van Hilten, and F. C. van der Helm, "Quantifying proprioceptive reflexes during position control of the human arm," *IEEE Trans Biomed Eng,* vol. 55, pp. 311-21, Jan 2008.

[19] F. C. van der Helm, A. C. Schouten, E. de Vlugt, and G. G. Brouwn, "Identification of intrinsic and reflexive components of human arm dynamics during postural control," *J Neurosci Methods,* vol. 119, pp. 1-14, Sep 15 2002.

[20] J. Lataire, R. Pintelon, and E. Louarroudi, "Non-parametric estimate of the system function of a time-varying system," *Automatica,* vol. 48, pp. 666-672, Apr 2012.

[21] S. H. Scott, "Optimal feedback control and the neural basis of volitional motor control," *Nat Rev Neurosci,* vol. 5, pp. 532-46, Jul 2004.

[22] E. Todorov and M. I. Jordan, "Optimal feedback control as a theory of motor coordination," *Nat Neurosci,* vol. 5, pp. 1226-35, Nov 2002.

[23] J. Shemmell, M. A. Krutky, and E. J. Perreault, "Stretch sensitive reflexes as an adaptive mechanism for maintaining limb stability," *Clin Neurophysiol,* vol. 121, pp. 1680-9, Oct 2010.

[24] M. A. Krutky, V. J. Ravichandran, R. D. Trumbower, and E. J. Perreault, "Interactions between limb and environmental mechanics influence stretch reflex sensitivity in the human arm," *J Neurophysiol,* vol. 103, pp. 429-40, Jan 2010.